The slab ocean El Niño

Dietmar Dommenget[1]

Received 28 July 2010; revised 2 September 2010; accepted 3 September 2010; published 16 October 2010.

[1] In a series of Atmospheric model simulations coupled to a simple slab ocean model it is illustrated that El Niño type of SST variability can exist in the absence of any ocean dynamics. Atmospheric feedbacks in cloud cover and changes in the wind field can produce positive and delayed negative feedbacks that together with the heat capacity of the upper ocean can produce a damped interannual oscillation in the equatorial Pacific that is comparable in strength and has characteristics to the observed phenomenon. The evolution of the SST pattern is similar to the SST-mode of El Niño, but is entirely controlled by atmospheric feedbacks. The results challenge and extend our current understanding of the feedback mechanisms of El Niño in climate models and may also highlight possible atmospheric mechanisms that could partly control some observed ENSO events. **Citation:** Dommenget, D. (2010), The slab ocean El Niño, *Geophys. Res. Lett.*, *37*, L20701, doi:10.1029/2010GL044888.

1. Introduction

[2] The El Niño/Southern Oscillation (ENSO) Mode is the globally dominating mode of interannual climate variability, which is generally assumed to be caused by the interaction between the atmospheric circulation over the tropical Pacific and the tropical Pacific upper ocean dynamics [e.g., *Jin*, 1997; *Neelin et al.*, 1998]. Ocean dynamics essentially control ENSO events, by controlling the positive Bjerknes and delayed negative feedbacks, involving oceanic Rossby and Kelvin waves that control the evolution of an ENSO events. It has thus been assumed that the ENSO mode cannot be simulated in a climate model without ocean dynamics.

[3] A series of simulations with the ECHAM5 atmosphere coupled to slab oceans are discussed in this study, in which El Niño-type of variability exist. Slab oceans by construction do not simulate any kind of ocean dynamics.

2. Slab Ocean Models

[4] The simulations analyzed in this study are based on the ECHAM5 atmosphere model in T31 (3.75° × 3.75°) horizontal resolution, which is a fully complex atmospheric GCM [*Roeckner et al.*, 2003]. The sea surface temperature (SST) is simulated by a simple slab ocean model for open ocean conditions and by a simple thermo dynamical sea ice model for sea ice conditions. In a slab ocean the SST heat balance is only caused by atmospheric heat fluxes and some prescribed, seasonally varying, but state independent ocean heat fluxes, F_{ocean}, mimicking ocean heat transport. Slab ocean models are used in many different studies as a first order approximation of SST variability or response to external forcings [e.g., *Washington and Meehl*, 1984; *Dommenget and Latif*, 2002; *Murphy et al.*, 2004].

[5] By controlling F_{ocean} the SST climatology in the simulations is forced to closely follow any given SST climatology. The set of simulations discussed in this study is based on 24 simulations, each 50 yrs long, with 24 different SST climatologies taken from the 24 models of the 20th century scenario in the CMIP3 database [*Meehl et al.*, 2007] (here referred to as SLAB simulations). One of the 24 simulations is continued for 1000 yrs (referred to as SLAB-ELNINO). Two additional simulations with the same SST climatology, but the mixed layer depth of 20 m (SLAB-20M) and 100 m (SLAB-100M), instead of the 50 m depth used in all other simulations have been integrated over 400 years each.

3. Slab Ocean El Niño

[6] In the SLAB simulations most members show the typical SST standard deviation [e.g., see *Dommenget and Latif*, 2002] of slab ocean models, with the absence of the observed strong SST variability in the equatorial Pacific and increasing SST variability with latitudes as atmospheric heat flux variability is increasing, see Figure 1a. However, a subset of 5 members shows unexpectedly strong SST variability in the equatorial Pacific, which is even slightly stronger than observed (Figure 1b). The time series of SST in the NINO3 (150°W–90°W, 5°S–5°N) region of the longer SLAB-ELNINO simulation shows strong stochastic interannual variability with maximum power on 5 to 8 years period, see Figures 1c and 1d. The SST variability in this simulation shows clear signs of non-linearity, with strong negative skewness, whereas the set of "El Niño Off" simulations shows a normal (linear) probability distribution function, see Figure 1e.

[7] The 24 SLAB simulations differ to each other only in the F_{ocean} boundary condition and therefore only in the SST climatology interacting with the atmosphere. The set with "El Niño On" conditions has a much stronger (>99% confidence level of the students t-test) equatorial cold tongue condition, than the set with "El Niño Off" conditions, see Figures 1f and 1g. Analysis of the climatologies of the SLAB simulations shows, that the much stronger cold tongue, along with a slightly more symmetric meridional structure enhances the meridional temperature gradient, decreases the atmospheric water vapor over the equatorial Pacific, decreases the total cloud cover over the western equatorial Pacific and changes the surface winds to blow more strongly away from the equator, which further supports the strong meridional temperature gradient. This leads to a highly unstable mean state in the NINO3 region with a

[1]School of Mathematical Sciences, Monash University, Clayton, Victoria, Australia.

0094-8276/10/2010GL044888

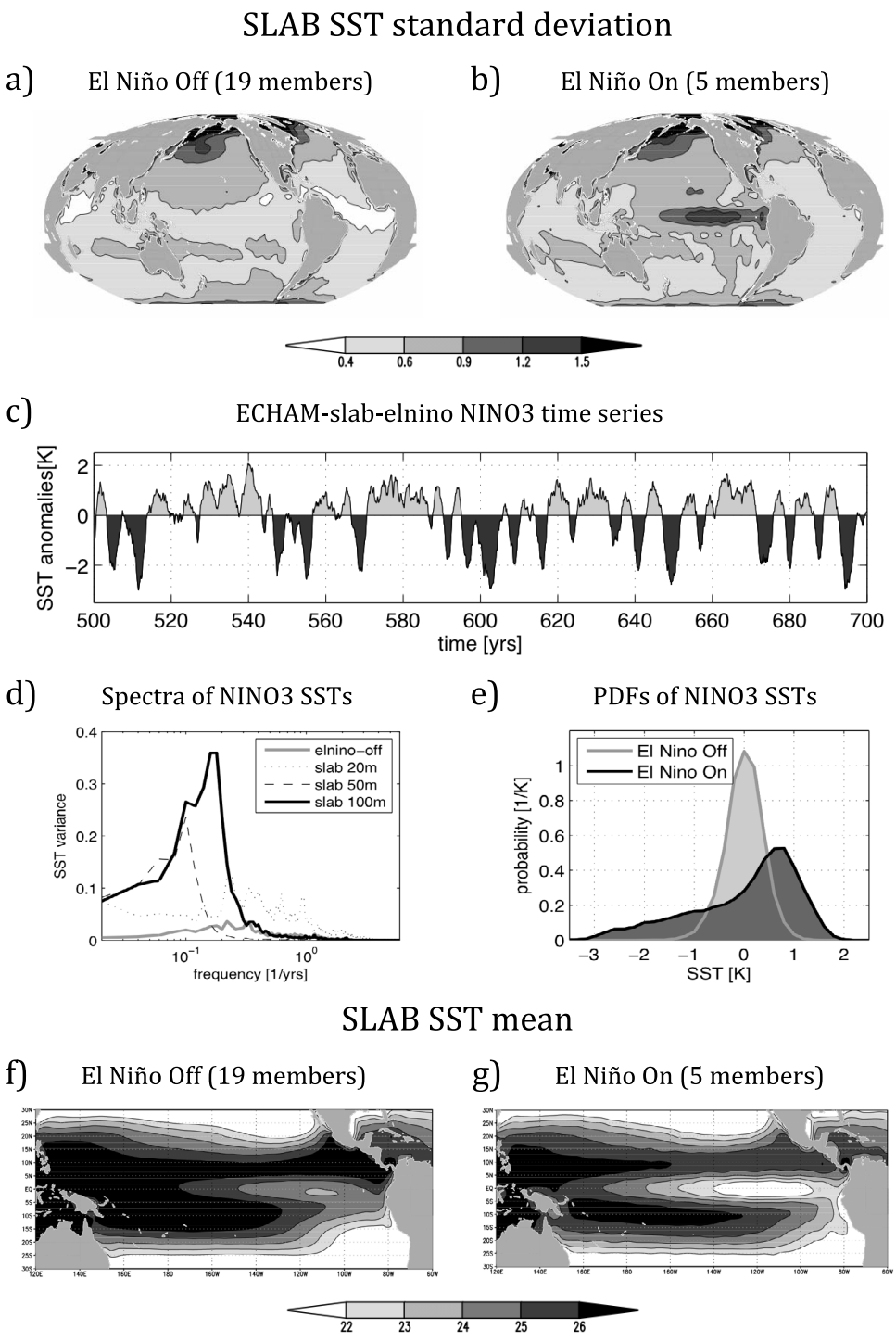

Figure 1. (a) the mean standard deviation for all slab simulations with the NINO3 SST stdv <0.8 K. (b) As Figure 1a, but for NINO3 SST stdv >0.8 K. (c) Time series section of the NINO3 SST anomalies in the ECHAM-slab-elnino simulation. (d) The spectra of NINO3 SST anomaly time series of different simulations. (e) The histograms of NINO3 SST anomaly time series of different simulations. (f) As Figure 1a but for the mean SST, (g) as Figure 1b but for the mean SST.

feedback sensitivity (estimated with a least square fit to the monthly mean tendencies of the SST assuming a first order linear damping approximation for the tendencies: $\gamma\frac{dSST}{dt} = \frac{1}{\lambda}SST$, with the heat capacity of the slab ocean, γ) of about 1 K/(W/m^2), which is much larger than in the "El Niño Off" mean states (about 0.2 K/(W/m^2)).

[8] The mean evolution of an El Niño event in the SLAB-ELNINO simulation is shown in Figure 2a. The initial SST anomaly forms off the coast of South America, south of the equator, then propagates to the west and amplifies along the equator until it covers almost the entire equatorial Pacific and then starts to decay.

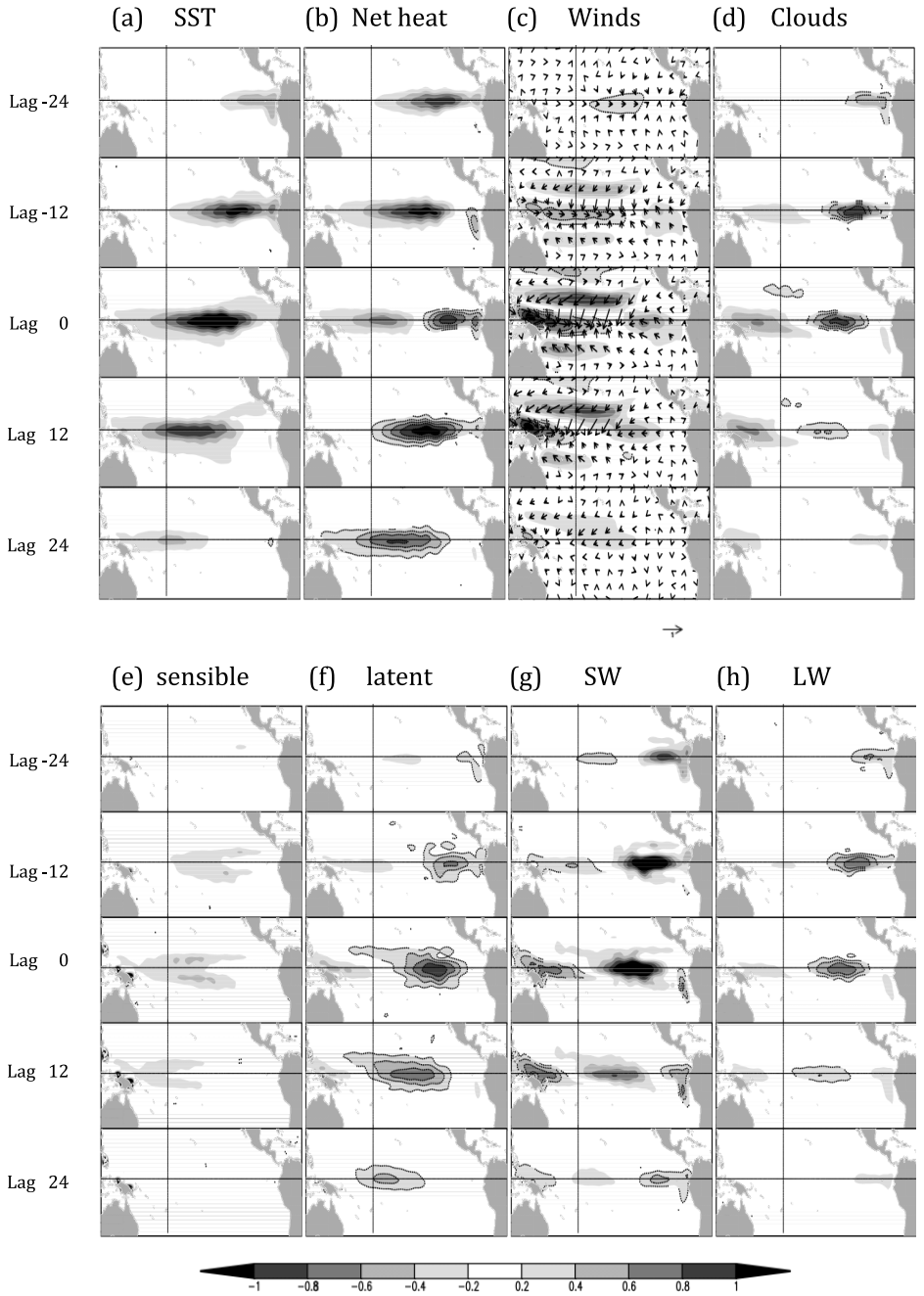

Figure 2. Lag-lead [month] regression between the SST at 150°W, 0°N and (a) the SST [1.5 K/K], (b) the net heat flux [7 W/K/m^2], (c) 10 m wind vectors and absolute values [1 m/s/K], (d) cloud cover [0.2/K], (e) sensible heat flux [7 W/K/m^2], (f) latent heat flux [20 W/K/m^2], (g) short wave [20 W/K/m^2] and (h) long wave [20 W/K/m^2] radiation field. Contour lines in all panels mark negative values.

[9] The anomalous SST tendencies in the slab ocean models are entirely caused by the net atmospheric heat fluxes (Figure 2b). Understanding the atmospheric feedbacks causing the El Niño events can be based on the four components that contribute to the net heat flux, see Figures 2e–2h. We can first of all recognize that the amplitudes of the latent, short wave and long wave heat flux components are much larger, than the net heat flux, indicating that the individual heat flux components, and associated feedback mechanisms, are strongly counter acting each other.

[10] In the initial phase of the El Niño event the net tendencies are dominated by the short wave heat fluxes on top of the SST anomaly peak. The westward propagation is caused by a superposition of positive latent, long wave and sensible heat fluxes to the west of the SST anomaly peak. In the mature phase the westward propagation is additionally forced by negative latent and long wave heat fluxes to the east of the SST anomaly peak. In the decaying phase latent and long wave heat fluxes combined dominate the negative SST tendencies.

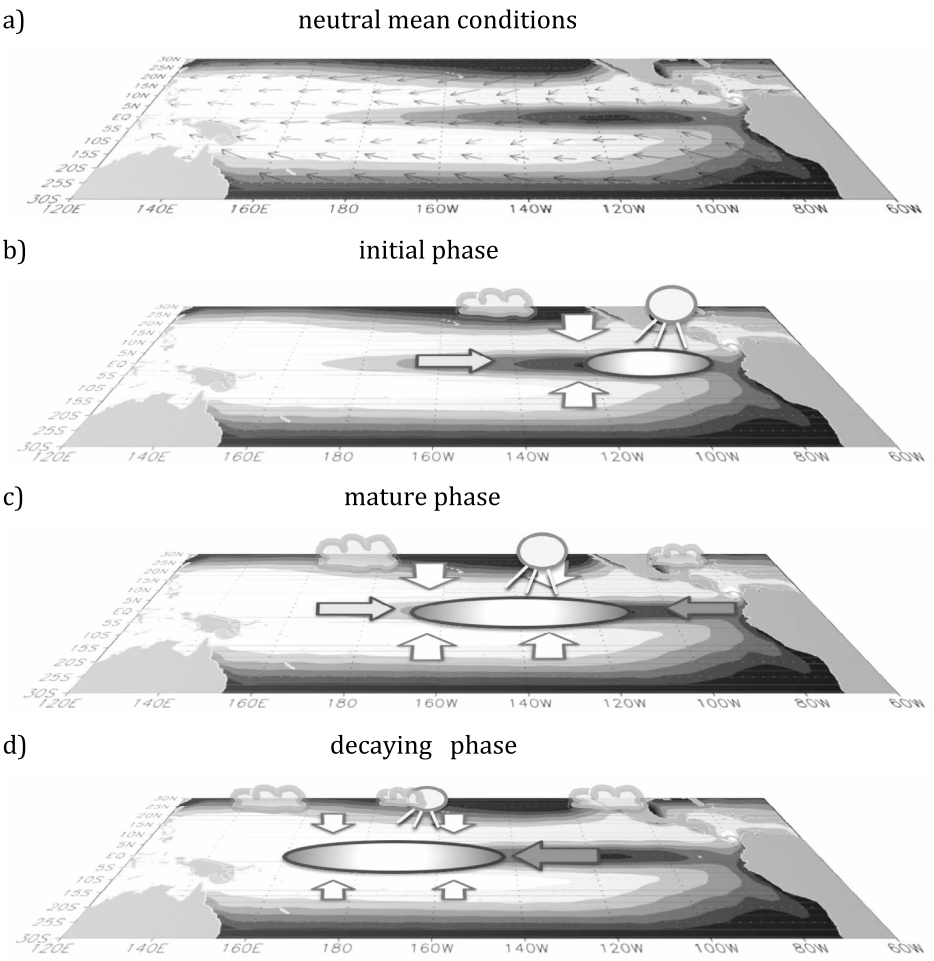

Figure 3. Sketch illustrating the evolution of an El Niño event in the SLAB-ELNINO simulation. Arrows, clouds and sun indicate changes in the winds, cloud cover and incoming short wave radiation. Winds, which lead to warming/cooling, are light/dark arrows.

[11] The evolution of the El Niño events are entirely forced by atmospheric processes, we can therefore describe it by a simple sketch of the evolution of the atmospheric conditions during the phases of a typical El Niño event, see Figure 3. In neutral conditions, the equatorial Pacific has the mean winds blowing easterly and away from the equator (Figure 3a), and some moderate mean total cloud cover is present. The equatorial SST is much colder than those of the nearby higher latitudes on both hemispheres.

[12] When an SST anomaly develops in the eastern coastal equatorial Pacific the winds converge over the SST anomaly, as known for a Gill-type response [*Matsuno*, 1966; *Gill*, 1980]. In addition some weak reduced easterly winds are present to the west along the equatorial Pacific (Figure 3c). Changes in the atmospheric circulations go along with reduced cloud cover on top of the SST anomaly, which enhances the absorbed short wave radiation. The reduced cloud cover is the main driver for the initial amplification of the SST anomaly (see SW heat in Figure 2e). The reduced winds to the west reduce the latent heat loss and the wind convergence leads to anomalous heat advection from higher and warmer latitudes and subsequently to positive sensible heat fluxes to the west of the SST anomaly. A slight increase in cloud cover to the west reduces the long wave heat loss, which also contributes to the overall positive heat fluxes to the west of the initial SST anomaly. These elements together lead to a westward extension of the initial SST anomaly to the central Pacific.

[13] When the El Niño event has reached the central equatorial Pacific, the reduced cloud cover on top of the SST peak still amplifies the SST anomaly. The zonal winds are now converging onto the SST anomaly from both sides, causing warming to the west by both reduced wind speed and latent heat loss and causing cooling to the east by both enhanced easterlies and latent heat loss, which erodes the SST anomaly from the east, supporting the further westward propagation of the signal.

[14] Once the SST anomaly is centered more to the western side of the equatorial Pacific the short wave amplification by reduced clouds weakens, but still amplifies the SST anomaly. The winds are still converging over the SST anomaly, but now the enhanced easterlies to the east of the peak are the more dominant signal, causing a dominant increase in latent heat loss. This dominates the SST tendencies, leading to the decay of the signal.

[15] The timescale of the El Niño oscillation period is controlled by the positive and negative feedbacks and the inertia of the system. The time needed to build up the SST signal and to propagate to the west depends on both the strength of the net heat responds and the heat capacity of the

ocean. The strength of the net heat flux responds is controlled by the sensitivity and balances of different competing processes in the atmosphere (e.g. cloud cover or winds), which are a result of the mean state climate. If the heat capacity of the slab ocean is changed from 50 m to 100 m or 20 m, the timescale of the NINO3 SST variability changes accordingly, see Figure 1d. A doubling of the heat capacity (100 m) leads to an approx. doubling of the timescale (center of mass of the power spectrum in Figure 1e) and a reduction to 20 m approx. lead to a similar reduction in the time scale of El Niño.

4. Conclusions and Discussions

[16] The slab ocean simulations in summary illustrate that El Niño-type of SST variability can exist entirely controlled by atmospheric feedbacks and ocean heat capacity. This type of variability tends to only exist if the equatorial Pacific cold tongue is strong, supporting an unstable balance of atmospheric feedbacks between clouds and circulation changes. The SST variability is an east to west propagation, which is similar to the 'SST mode' of ENSO described in theoretical studies [e.g., *Neelin*, 1991; *Neelin et al.*, 1998; *Fedorov and Philander*, 2001]. However, while the 'SST mode' in previous studies was considered to be controlled by oceanic processes, the mode described here differs from that, as it is entirely controlled by atmospheric short wave, sensible and latent heat forcing, whose timescale is controlled by the strength of the atmospheric feedbacks and the heat capacity of the surface ocean layer.

[17] While the results indicate that atmospheric processes only could potentially explain aspects of the ENSO mode that is not to say that ocean processes and dynamics are not important. In fact observed ENSO events are strongly controlled by ocean dynamics [e.g., *Jin*, 1997; *Neelin et al.*, 1998]. Even more importantly ocean dynamics control to the largest part the mean state of the SST (equation cold tongue), which is a key element of the SLAB-ELNINO ENSO mode that forces the unstable atmospheric mean state. The results rather suggest that the atmospheric processes seen in the SLAB-ELNINO simulations may play a more important role in controlling amplitude, timescale and dynamics of the El Niño events, than it has been shown so far. These processes may somewhat be masked by the more dominant ocean dynamics, but may in some ENSO events or over some time period in the past or future be of importance. Indeed atmospheric heat fluxes in the NCEP reanalysis data [*Kalnay et al.*, 1996] are mostly negative during ENSO events, but some elements are positive: the net heat flux over the peak of the ENSO anomaly tends to be positive in the developing phase and the sensible heat flux over the central Pacific tends to be positive during the peak phase too, which is similar to the ENSO events discussed in this study.

[18] In the light of these results it is also interesting to study the ENSO mode in coupled climate models, which have strong differences to the observed and also vary very much between different models. Much of the difference in these coupled models may result from different SST mean states and differences in the simulation of atmospheric processes, such as cloud cover, which are very uncertain in current climate models. Some of the ENSO modes in climate models may indeed be more similar to the atmospheric ENSO mode describe in this study, than to the observed ocean forced ENSO mode. Indeed some of the early models tend to have westward propagating SST anomalies similar to those described in this study [*Neelin et al.*, 1992].

[19] **Acknowledgments.** I like to thank Alexey Fedorov, Tony Hirst, Noel Keenlyside, Mojib Latif and Matt Wheeler for discussions and comments.

References

Dommenget, D., and M. Latif (2002), Analysis of observed and simulated SST spectra in the midlatitudes, *Clim. Dyn.*, *19*, 277–288, doi:10.1007/s00382-002-0229-9.

Fedorov, A. V., and S. G. Philander (2001), A stability analysis of tropical ocean-atmosphere interactions: Bridging measurements and theory for El Niño, *J. Clim.*, *14*, 3086–3101, doi:10.1175/1520-0442(2001)014<3086:ASAOTO>2.0.CO;2.

Gill, A. E. (1980), Some simple solutions for heat-induced tropical circulation, *Q. J. R. Meteorol. Soc.*, *106*, 447–462, doi:10.1002/qj.49710644905.

Jin, F. F. (1997), An equatorial ocean recharge paradigm for ENSO. 1. Conceptual model, *J. Atmos. Sci.*, *54*, 811–829, doi:10.1175/1520-0469(1997)054<0811:AEORPF>2.0.CO;2.

Kalnay, E., et al. (1996), The NCEP/NCAR 40-year reanalysis project, *Bull. Am. Meteorol. Soc.*, *77*, 437–471, doi:10.1175/1520-0477(1996)077<0437:TNYRP>2.0.CO;2.

Matsuno, T. (1966), Quasi-geostrophic motions in the equatorial area, *J. Meteorol. Soc. Jpn.*, *44*, 25–43.

Meehl, G. A., C. Covey, T. Delworth, M. Latif, B. McAvaney, J. F. B. Mitchell, R. J. Stouffer, and K. E. Taylor (2007), The WCRP CMIP3 multimodel dataset: A new era in climate change research, *Bull. Am. Meteorol. Soc.*, *88*, 1383, doi:10.1175/BAMS-88-9-1383.

Murphy, J. M., D. M. H. Sexton, D. N. Barnett, G. S. Jones, M. J. Webb, and M. Collins (2004), Quantification of modelling uncertainties in a large ensemble of climate change simulations, *Nature*, *430*, 768–772, doi:10.1038/nature02771.

Neelin, J. D. (1991), The slow sea-surface temperature mode and the fast-wave limit: Analytic theory for tropical interannual oscillations and experiments in a hybrid coupled model, *J. Atmos. Sci.*, *48*, 584–606, doi:10.1175/1520-0469(1991)048<0584:TSSSTM>2.0.CO;2.

Neelin, J. D., et al. (1992), Tropical air-sea interaction in general-circulation models, *Clim. Dyn.*, *7*, 73–104, doi:10.1007/BF00209610.

Neelin, J. D., D. S. Battisti, A. C. Hirst, F.-F. Jin, Y. Wakata, T. Yamagata, and S. E. Zebiak (1998), ENSO theory, *J. Geophys. Res.*, *103*(C7), 14,261–14,290, doi:10.1029/97JC03424.

Roeckner, E., et al. (2003), The atmospheric general circulation model ECHAM 5. Part I: Model description, *Rep. 349*, Max-Planck-Inst. for Meteorol., Hamburg, Germany.

Washington, W. M., and G. A. Meehl (1984), Seasonal cycle experiment on the climate sensitivity due to a doubling of CO_2 with an atmospheric general circulation model coupled to a simple mixed-layer ocean model, *J. Geophys. Res.*, *89*(D6), 9475–9503, doi:10.1029/JD089iD06p09475.

D. Dommenget, School of Mathematical Sciences, Monash University, Clayton, Vic 3800, Australia. (dietmar.dommenget@monash.edu)